

to measure the distortion and bitrate. For distance function $d(\mathbf{x}, \hat{\mathbf{x}})$, MSE (Mean-Squared Error), $\text{PSNR} = 10 \cdot \log_{10}(\frac{\text{MAX}_L^2}{\text{MSE}})$ (Peak Signal-to-noise Ratio), $\text{SSIM}(\mathbf{x}, \hat{\mathbf{x}}) = \frac{(2\mu_{\mathbf{x}}\mu_{\hat{\mathbf{x}}} + (k_1 L)^2)(2\sigma_{\mathbf{x}\hat{\mathbf{x}}} + (k_2 L)^2)}{(\mu_{\mathbf{x}}^2 + \mu_{\hat{\mathbf{x}}}^2 + (k_1 L)^2)(\sigma_{\mathbf{x}}^2 + \sigma_{\hat{\mathbf{x}}}^2 + (k_2 L)^2)}$ (Structural Similarity Index) and MS-SSIM (Multiscale SSIM) are the most widely used metrics. For the entropy estimator H , apart from the GSM model mentioned in the former section, recent works also use generative models[5] and context models[8] as potential alternatives. For works of non-autoencoder approaches, there is also an increasing interest in the usage of GAN [9], GDN (Generalized Divisive Normalization) [5] and RNN [10].

The traditional convex optimization ADMM algorithm [11] first saw its application in the field of neural architecture search (NAS) by the method proposed by Han et al. [12], which is followed by a few improvements in [13, 14, 15].

3. PROPOSED METHOD

A typical CAE consists of an encoder E , a decoder D and a quantizer Q [1]:

$$\begin{aligned} E &: \mathbb{R}^n \rightarrow \mathbb{R}^m, \\ D &: \mathbb{R}^m \rightarrow \mathbb{R}^n, \\ Q &: \mathbb{R}^m \rightarrow \mathbb{Z}^m. \end{aligned}$$

The encoder E maps the original image $\mathbf{x} \in \mathbb{R}^n$ to a latent representation $\mathbf{z} = E(\mathbf{x})$. The quantizer Q then maps each element of \mathbf{z} to \mathbb{Z} , which produces the compressed presentation of the image $\hat{\mathbf{z}} = Q(\mathbf{z})$. Finally, the decoder D attempts to reconstruct the original image $\hat{\mathbf{x}} = D(\hat{\mathbf{z}})$ from the information in $\hat{\mathbf{z}}$.

We aim to let the reconstructed image $\hat{\mathbf{x}}$ looks as similar as the original \mathbf{x} (minimize the distance function d) while reducing the number of bits needed to store the latent code, or minimize the bitrate R . The problem can then be rephrased as below, assuming that Q is not parameterized:

$$\argmin_{E,D} d(\mathbf{x}, D \circ Q \circ E(\mathbf{x})) + \beta \cdot R \circ Q \circ E(\mathbf{x}) \quad (2)$$

3.1. Selection of E , D and Q

Similar to [1], CAE-ADMM uses convolutional layers to be the basis of our encoder and decoder. The decoder mirrors the structure of the encoder to maintain symmetry, except that uses sub-pixel convolutional layers proposed by Shi et al.[16] to perform up-sampling.

For the quantizer Q , we use a simple and computationally efficient one proposed by Theis et al.[1], inspired by the random binary version developed by Torderici et al.[10]. It is defined as:

$$Q(t) = \lfloor t \rfloor + \epsilon, \epsilon \in \{0, 1\}, \quad (3)$$

in which ϵ decides whether to output the ground or the ceiling of the input, and the probability of $\epsilon = 1$ satisfies $P(\epsilon = 1) = t - \lfloor t \rfloor$. To make the quantizer differentiable, we define its gradient with that of its expectation:

$$\frac{\partial}{\partial t} Q(t) = \frac{\partial}{\partial t} \mathbb{E}[Q(t)] = \frac{\partial}{\partial t} t = 1 \quad (4)$$

3.2. Solution to the optimization problem

Since multiple well-defined metrics (mentioned in section 2) exist for d , we here aim to provide an alternative method to optimize R without the use of H . Intuitively, we can reformulate R by

$$R(\hat{\mathbf{z}}) = \text{card}(\hat{\mathbf{z}}) = \text{card}(Q \circ E(\mathbf{x})), \quad (5)$$

in which $\text{card}(\cdot)$ counts the number of non-zero elements. If we want \mathbf{z} generated by the encoder to have fewer number of non-zero elements than a desired number ℓ , we can rephrase the problem into an ADMM-solvable problem [17]:

$$\begin{aligned} \argmin_{E,D} d(\mathbf{x}, \hat{\mathbf{x}}) + g(\mathbf{Z}), \\ \text{s.t. } Q \circ E(\mathbf{x}) - \mathbf{Z} = 0. \end{aligned} \quad (6)$$

where the indicator function $g(\cdot)$ is defined as

$$g(\mathbf{Z}) = \begin{cases} 0 & \text{if } \text{card}(\mathbf{Z}) \leq \ell, \\ +\infty & \text{otherwise.} \end{cases} \quad (7)$$

Remark that both \mathbf{U} and \mathbf{Z} are initialized to be all-zero, and \mathbf{Z} is an element of $\mathbf{S} = \{\mathbf{Z} | \text{card}(\mathbf{Z}) \leq \ell\}$. By introducing the dual variable \mathbf{U} and a penalty factor $\rho > 0$, we can split the above problem into two sub-problems. The first sub-problem is:

$$\argmin_{E,D} d(\mathbf{x}, \hat{\mathbf{x}}) + \frac{\rho}{2} \|Q \circ E(\mathbf{x}) - \mathbf{Z}^k + \mathbf{U}^k\|_F^2, \quad (8)$$

in which k is the current iteration number and $\|\cdot\|_F^2$ is the Frobenius norm. This is the neural network's loss with L_2 regularization, which can be solved by back propagation and gradient descent. The second sub-problem is:

$$\argmin_{\mathbf{Z}} g(\mathbf{Z}) + \frac{\rho}{2} \|Q^{k+1} \circ E^{k+1}(\mathbf{x}) - \mathbf{Z} + \mathbf{U}^k\|_F^2. \quad (9)$$

The solution to this problem was derived by Boyd et al. in 2011[18]:

$$\mathbf{Z}^{k+1} = \Pi_{\mathbf{S}}(Q^{k+1} \circ E^{k+1}(\mathbf{x}) + \mathbf{U}^k), \quad (10)$$

where $\Pi_{\mathbf{S}}(\cdot)$ represents the Euclidean projection onto the set \mathbf{S} . Generally, Euclidean projection onto a non-convex set is difficult, but Boyd et al.[18] have proved that the optimal solution is to keep the ℓ largest elements of $Q^{k+1} \circ E^{k+1}(\mathbf{x}) +$

\mathbf{U}^k and set the rest to zero. Finally, we will update the dual variable \mathbf{U} with the following policy:

$$\mathbf{U}^{k+1} = \mathbf{U}^k + Q^{k+1} \circ E^{k+1}(\mathbf{x}) - \mathbf{Z}^{k+1}. \quad (11)$$

These three steps together form one iteration of the ADMM pruning method. Algorithm 1 shows the complete steps.

Algorithm 1 Pruning of CAE Based on ADMM

Input:

\mathbf{x} : A batch of input images;
 E, D : The encoder and decoder;
 Q : The quantizer;
 ℓ : The expected number of non-zero elements in $E(\mathbf{x})$;
 k_m : Max number of iterations.

Output:

E, D : Trained encoder and decoder;
 $\mathbf{U}, \mathbf{Z} \leftarrow$ zeroes with the same shape as $Q \circ E(\mathbf{x})$
for $1 \leq k \leq k_m$ **do**
 $E, D \leftarrow \operatorname{argmin}_{E, D} d(\mathbf{x}, \hat{\mathbf{x}}) + \frac{\ell}{2} \|Q \circ E(\mathbf{x}) - \mathbf{Z} + \mathbf{U}\|_F^2$;
 $\mathbf{Z} \leftarrow$ keep the ℓ largest elements in $Q \circ E(\mathbf{x}) + \mathbf{U}$ and set the rest to 0;
 $\mathbf{U} \leftarrow \mathbf{U} + Q \circ E(\mathbf{x}) - \mathbf{Z}$.
end for
return E, D

4. EXPERIMENT

4.1. Model architecture

Our model architecture, shown in Fig. 1, is a modification of CAE proposed by [1]. The encoder and decoder are composed of convolutional layers as described in Section 3.1. The input image is first down-sampled by three blocks with each containing a convolutional layer, a batch normalization layer and a PReLU layer. Following 15 residual blocks, two more down-sampling convolutional blocks with the last convolutional block are applied, generating \mathbf{z} . The quantizer Q then quantizes it and fed into the decoder whose architecture mirrors the encoder.

4.2. Training

We use the Adam optimizer [19] with the batch size set to 32 to solve the first sub-problem. Learning rate is set to $4 \cdot 10^{-3}$ and is halved each time the loss has not dropped for ten epochs. Every 20 epochs, the second and third steps of the ADMM pruning method is applied. The distance function used as a part of back-propagation is a linear combination of MSE and differentiable versions of PSNR/SSIM/MS-SSIM, and the training is first warmed up by a scaled MSE alone. The ratio of the number of elements to retain in step two is set to be 10%. To enable fine-grained tuning of bpp, we modify

the last layer of the encoder. All procedures are implemented in PyTorch and open-sourced¹. Each model is trained for 300 epochs on 4 NVIDIA GeForce GTX 1080Ti GPUs.

4.3. Datasets and preprocessing

We use BSDS500 [20] as the training set, which contains five hundred 481×321 natural images. The images are randomly cropped to 128×128 , horizontally and vertically flipped and then normalized. For the test set, we use the Kodak PhotoCD dataset², which contains twenty-four 768×512 images.

4.4. Results and discussion

We test CAE-ADMM (Our method), JPEG (implemented by libjpeg³) and JPEG 2000 (implemented by Kadadu Software⁴) on the Kodak PhotoCD dataset. For the distance metric, we use the open-source implementation of SSIM and MS-SSIM⁵.

Fig. 2 shows a comparison of the performance achieved by the mentioned methods on Kodak. Our method (CAE-ADMM) outperforms all the other methods in both SSIM and MS-SSIM, especially the original CAE which uses entropy coding. Note that the blue curve represents the RNN-based method proposed by Toderici et al. which is optimized without an entropy estimator.

In Fig. 3, we demonstrate the effect of different compression methods visually: the origin (top left), JPEG (top right), CAE-ADMM (ours, bottom left) and JPEG 2000 (bottom right). From the figure, we can see that JPEG breaks down under a bpp of 0.3 while that of CAE-ADMM and JPEG are still satisfactory.

Model	bpp	ratio of zeros
Before pruning	1.684 ± 0.012	$7.80\% \pm 3.44\%$
After pruning	1.257 ± 0.011	$17.65\% \pm 4.90\%$

Table 1. Bpp & proportion of zero elements in $\hat{\mathbf{z}}$ the total number of elements in $\hat{\mathbf{z}}$ before and after pruning. For both statistics, a 95% confidence interval is established with a sample size of 233 (size of the mixed dataset).

For ablation study, we test out the effectiveness of ADMM-module by applying the same training procedure to the same model, one with the pruning schedule and another without. Then, we calculate the average bpp as well as the ratio of zero elements in a mixed dataset (768×512 crops of images from Urban100 [22], Manga109 [22] and Kodak PhotoCD). Results can be seen in Table 1 and more direct visualization of a sample image can be found in Figure 4.

¹<https://github.com/JasonZHM/CAE-ADMM>

²<http://r0k.us/graphics/kodak/>

³<http://libjpeg.sourceforge.net/>

⁴<http://kakadusoftware.com/>

⁵<https://github.com/jorge-pessoa/pytorch-msssim>

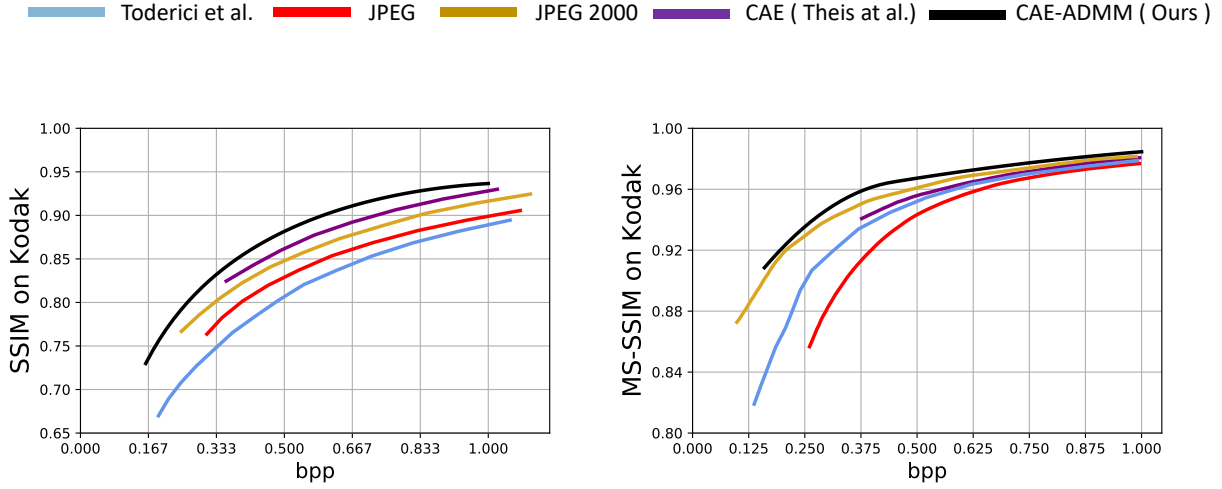


Fig. 2. Comparison of different method with respect to SSIM and MS-SSIM on the Kodak PhotoCD dataset. Note that Toderici et al.[21] used RNN structure instead of entropy coding while CAE-ADMM (Ours) replaces entropy coding with pruning method.



Fig. 3. Performance of different methods on image *kodim21* from Kodak dataset. Bpp is set to be about 0.3.

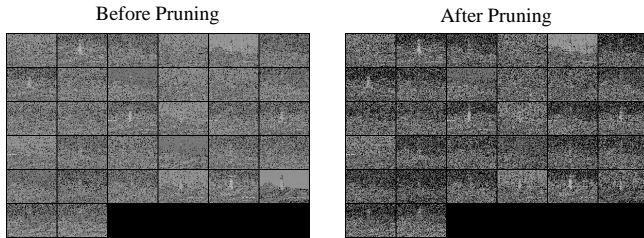


Fig. 4. Comparison of latent code before and after pruning for *kodim21*. For the sake of clarity, we marked zero values in the feature map before normalization as black.

Inference-speed-wise, from Table 2 we can see that our CAE-ADMM has an acceptable inference speed comparing to traditional codecs while maintaining superior quality concerning SSIM.

Model	$\overline{\text{bpp}}$	SSIM	Second/image
bpp_0.5	0.597	0.871\pm0.003	0.140 \pm 0.008
JPEG	0.603	0.828 \pm 0.006	0.033\pm0.001
JPEG2000	0.601	0.793 \pm 0.013	0.177 \pm 0.020

Table 2. 95% confidence intervals of SSIM and inference speed of CAE-ADMM model (inference time being the sum of all 128×128 patches with batch size = 8) on mixed dataset, 2 GPUs compared to traditional codecs.

5. CONCLUSION

In this paper, we propose the compressive autoencoder with ADMM-based pruning (CAE-ADMM) which serves as an alternative to the traditionally used entropy estimating technique for deep-learning-based lossy image compression. Tests on multiple datasets show better results than the original CAE model along with other contemporary approaches. We further explore the effectiveness of the ADMM-based pruning method by looking into the detail of learned latent codes.

Further study can focus on developing a more efficient pruning method, e.g., introducing ideas from the field of reinforcement learning. Also, the structures of E , D , and Q can be further optimized for speed and accuracy.

6. REFERENCES

- [1] Lucas Theis, Wenzhe Shi, Andrew Cunningham, and Ferenc Huszár, “Lossy image compression with compressive autoencoders,” *arXiv preprint arXiv:1703.00395*, 2017.
- [2] Gregory K Wallace, “The jpeg still picture compression standard,” *IEEE transactions on consumer electronics*, vol. 38, no. 1, pp. xviii–xxxiv, 1992.
- [3] David S. Taubman and Michael W. Marcellin, *JPEG 2000: Image Compression Fundamentals, Standards and Practice*, 2002.
- [4] Feng Jiang, Wen Tao, Shaohui Liu, Jie Ren, Xun Guo, and Debin Zhao, “An end-to-end compression framework based on convolutional neural networks,” *IEEE Transactions on Circuits and Systems for Video Technology*, 2017.
- [5] Johannes Ballé, Valero Laparra, and Eero P Simoncelli, “End-to-end optimization of nonlinear transform codes for perceptual quality,” in *Picture Coding Symposium (PCS), 2016*. IEEE, 2016, pp. 1–5.
- [6] Eirikur Agustsson, Fabian Mentzer, Michael Tschanen, Lukas Cavigelli, Radu Timofte, Luca Benini, and Luc V Gool, “Soft-to-hard vector quantization for end-to-end learning compressible representations,” in *Advances in Neural Information Processing Systems*, 2017, pp. 1141–1151.
- [7] Mu Li, Wangmeng Zuo, Shuhang Gu, Debin Zhao, and David Zhang, “Learning convolutional networks for content-weighted image compression,” *arXiv preprint arXiv:1703.10553*, 2017.
- [8] Fabian Mentzer, Eirikur Agustsson, Michael Tschanen, Radu Timofte, and Luc Van Gool, “Conditional probability models for deep image compression,” in *IEEE Conference on Computer Vision and Pattern Recognition (CVPR)*, 2018, vol. 1, p. 3.
- [9] Oren Rippel and Lubomir Bourdev, “Real-time adaptive image compression,” *arXiv preprint arXiv:1705.05823*, 2017.
- [10] George Toderici, Sean M O’Malley, Sung Jin Hwang, Damien Vincent, David Minnen, Shumeet Baluja, Michele Covell, and Rahul Sukthankar, “Variable rate image compression with recurrent neural networks,” *arXiv preprint arXiv:1511.06085*, 2015.
- [11] Stephen Boyd, Neal Parikh, Eric Chu, Borja Peleato, and Jonathan Eckstein, “Distributed optimization and statistical learning via the alternating direction method of multipliers,” *Found. Trends Mach. Learn.*, vol. 3, no. 1, pp. 1–122, Jan. 2011.
- [12] Song Han, Jeff Pool, John Tran, and William Dally, “Learning both weights and connections for efficient neural network,” in *Advances in neural information processing systems*, 2015, pp. 1135–1143.
- [13] Tien Ju Yang, Yu Hsin Chen, and Vivienne Sze, “Designing energy-efficient convolutional neural networks using energy-aware pruning,” pp. 6071–6079, 2017.
- [14] Yiwen Guo, Anbang Yao, and Yurong Chen, “Dynamic network surgery for efficient dnns,” vol. to appear, 2016.
- [15] Yihui He, Xiangyu Zhang, and Jian Sun, “Channel pruning for accelerating very deep neural networks,” 2017.
- [16] Wenzhe Shi, Jose Caballero, Ferenc Huszar, Johannes Totz, Andrew P. Aitken, Rob Bishop, Daniel Rueckert, and Zehan Wang, “Real-time single image and video super-resolution using an efficient sub-pixel convolutional neural network,” pp. 1874–1883, 2016.
- [17] Shaokai Ye, Tianyun Zhang, Kaiqi Zhang, Jiayu Li, Kaidi Xu, Yunfei Yang, Fuxun Yu, Jian Tang, Makan Fardad, Sijia Liu, et al., “Progressive weight pruning of deep neural networks using admm,” *arXiv preprint arXiv:1810.07378*, 2018.
- [18] Stephen Boyd, Neal Parikh, Eric Chu, Borja Peleato, and Jonathan Eckstein, “Distributed optimization and statistical learning via the alternating direction method of multipliers,” *Foundations & Trends in Machine Learning*, vol. 3, no. 1, pp. 1–122, 2011.
- [19] Diederik P Kingma and Jimmy Ba, “Adam: A method for stochastic optimization,” *arXiv preprint arXiv:1412.6980*, 2014.
- [20] David Martin, Charless Fowlkes, Doron Tal, and Jitendra Malik, “A database of human segmented natural images and its application to evaluating segmentation algorithms and measuring ecological statistics,” in *Computer Vision, 2001. ICCV 2001. Proceedings. Eighth IEEE International Conference on*. IEEE, 2001, vol. 2, pp. 416–423.
- [21] George Toderici, Damien Vincent, Nick Johnston, Sung Jin Hwang, David Minnen, Joel Shor, and Michele Covell, “Full resolution image compression with recurrent neural networks,” in *CVPR*, 2017, pp. 5435–5443.
- [22] Wei-Sheng Lai, Jia-Bin Huang, Narendra Ahuja, and Ming-Hsuan Yang, “Fast and accurate image super-resolution with deep laplacian pyramid networks,” *arXiv:1710.01992*, 2017.